RSC Advances

ROYAL SOCIETY OF CHEMISTRY

www.rsc.org/advances

Journal Name

ARTICLE

Large-Scale R2R Fabrication of Piezoresistive Films (Ni/PDMS) with Enhanced through thickness Electrical and Thermal properties by Magnetic field

Received 00th January 20xx,
Accepted 00th January 20xx

DOI: 10.1039/x0xx00000x

www.rsc.org/

Yuwei Chen[a,b], Yuanhao Guo[a], Saurabh Batra[a], Emre Unsal[a], Enmin Wang[a], Yanping Wang[b], Xueqing Liu[c], Yimin Wang[b], Miko Cakmak[a]*

The first successful development of a roll to roll (R2R) process that applies external magnetic field to orient and organize magnetic nanoparticles along nanocolumns in thickness direction of thin films to obtain high electrical and thermal conductivities in thickness direction is reported. Utilizing the R2R machine that includes in-line electromagnet, we orient and organize Ni nanoparticles in nanocolumns inside a flexible Poly(dimethylsiloxane) matrix. In these films, nanocolumns of Ni particles point in the magnetic field/ thickness direction that leads to enhancement of electrical and thermal conductivity in thickness direction while maintaining optical transparency as the space between the nanocolums are depleted of nanoparticles facilitating unimpeded light transmission. Exhibiting piezoresistivity, the electrical conductivity in these films increases by as much as 7 orders under moderate pressures. The thermal conductivity of aligned composite films filled with 14 vol. % Ni flakes was found to increase 50 times the conductivity of polymer matrix, or 13 times the conductivity of non-aligned composite of the same concentration. This R2R method facilitates the manufacture of unique films with enhanced functional properties in thickness direction to be used in a range of including Z direction heat spreaders, transparent switches, privacy protection screens and piezoresistive sensors.

Introduction

As electronics become thinner and more flexible, the demand on the properties of their components increases particularly for their multifunctionality[1, 2]. In the past decade, a great deal of research has been devoted to obtain organization and preferred orientation of particles and disperse phases in polymer films, creating beneficial thickness direction ("Z") anisotropy that is not commonly achievable by traditional polymer film processing operations. Oriented pathways can be created through directional alignment to enhance the selectivity and flux of polymer films for various applications such as sensors, heat spreaders, slow electric discharge microelectronic packaging, ultrahigh density information storage systems, capacitors, solar cells, ion exchange, and fuel cell membranes[3-5].

Alignment and assembly of particles or phases has been studied previously, usually by the application of electric fields[6-10], magnetic fields[11-18], shear force[19-21], thermal gradient[22-24]. Magnetic fields are particularly attractive for realization of an externally imposed magnetic driving force in any shape mold without any geometrical constraints encountered with either electric field or mechanical shear, moreover, the general space pervasive nature of magnetic field enables formation of "Z" (thickness direction) aligned structures in thin film geometries

[a] Polymer Engineering Department, The University of Akron, Akron OH 44325-0301, USA.
[b] State Key Laboratory for Modification of Chemical Fibers and Polymer Materials, College of Materials Science and Engineering, Donghua University, Shanghai 201620, PR China.
[c] Key Laboratory of Optoelectronic Chemical Material and Devices of Ministry of Education, Jianghan University, Wuhan 430056, PR China.
† Footnotes relating to the title and/or authors should appear here.
Electronic Supplementary Information (ESI) available: [details of any supplementary information available should be included here]. See DOI: 10.1039/x0xx00000x

in the absence direct contact with electrodes and does not have upper electrical operational limitations caused by breakdown in electric fields[25, 26].

The mechanism and magnetic field-induced assembly of molecular chains[27-29], phase[25, 30], diamagnetic anisotropy[11, 31, 32], ferromagnetism in Nickel, cobalt, iron[2, 33, 34], have been well investigated. The main driver for ferromagnetic particles for alignment in external field along the nanocolumns made up of entrained particles in order to lower magnetostatic energy in a unidirectional magnetic field[33, 34]. Particles form chains due to the magnetic dipole-dipole attraction induced by the external magnetic field[35]. Magnetic field-induced alignment of non-ferromagnetic system only can proceed at relatively high magnetic fields to provide required driving force to reorientation since the anisotropy of susceptibility is usually a vanishingly small number. However, relatively low magnetic field is required for aligning ferromagnetic particles in polymer matrix since the magnetic susceptibility of ferromagnetic particles are far higher than the non-ferromagnetic ones. Therefore magnetic field-induced alignment of ferromagnetic particles is an effective and low cost pathway to ordered morphology and high conductivity at relatively low particle loading.

There are few reports on particle alignment to obtain anisotropic electrical and thermal conductivity. Knaapila and co-workers[2] aligned Ni particles in polymer matrix by placing the uncured samples between two rectangular oppositely placed magnets. The uniformly distributed particles are aligned by a magnetic field to form chainlike pathways through the sample that make the material directionally conductive and reversibly piezoresistive. Another prominent example was provided by Jin and co-workers[33], who aligned silver coated-Ni spheres in a thin layer of transparent polymer and formed chain-of-spheres configuration under a vertical magnetic field. When the polymer was solidified, the resultant composite contained vertically aligned but laterally isolated columns of particles. The sheet material is highly anisotropic in both optical and electrical properties. However, the batch methods used in these studies are not suited for mass production.

In order to realize large-scale continuous fabrication of vertically oriented Ni particles in PDMS by aligning Ni in PDMS assisted by magnetic field, we developed R2R line where the 6" wide non-magnetic metal carrier passes through the gap between the two poles of an electromagnet that is equipped with an air heating mechanism.

In this paper, we investigate the alignment behavior of Ni nanoparticles and nanoflakes dispersed in PDMS matrix continuously by applying magnetic field to form number of conductive paths along thickness direction in the polymer matrix to obtain functional films with enhanced through thickness electrical and thermal conductivities. This anisotropic structure is more sensitive to the applied pressure than uniform composite films, thereby resulting in a sharper positive stress coefficient effect of composite resistance.

Results and Discussion

Morphology of Aligned Nanocomposites

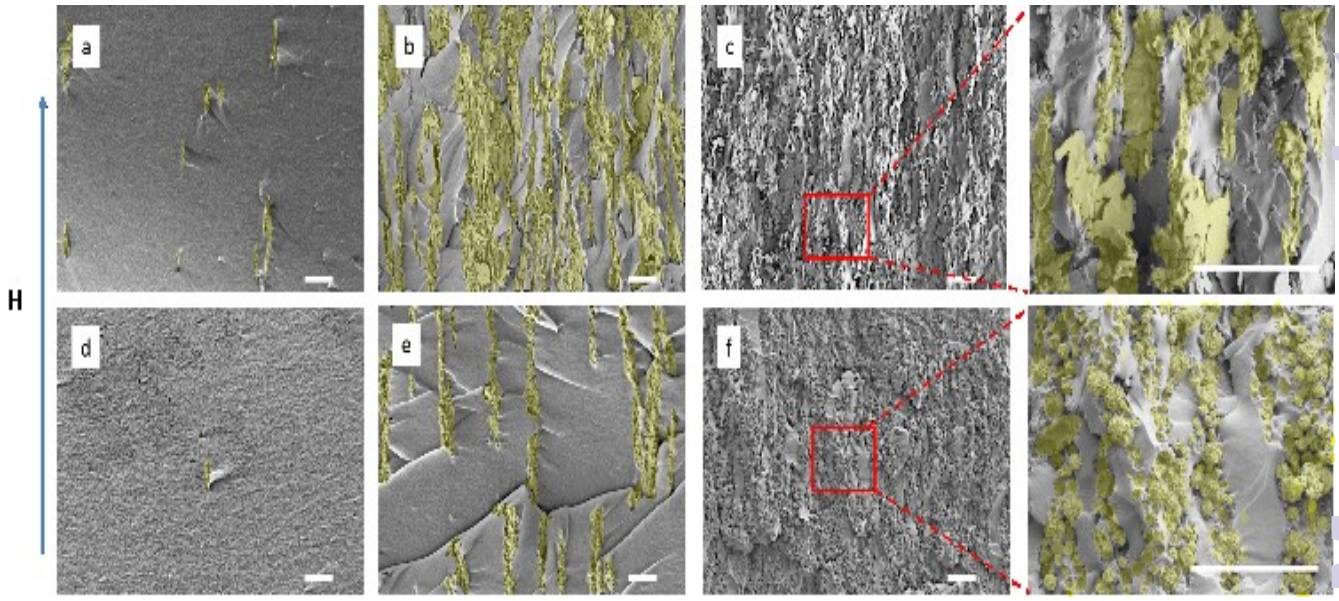

Fig. 1 Scanning electron micrograph of Ni/PDMS anisotropic composites film obtained by magnetic alignment. a, b, c, show Ni flakes aligned in PDMS with various loading at 0.11 vol.%, 2.45 vol.%, 14 vol.% respectively. d, e, f, shows Ni powder aligned in PDMS with 0.11 vol.%, 2.45 vol.%, 14 vol.% respectively. (Scale bar: 50um. H =200mT, nickel particles are shown with false color)

Ni particles can easily be magnetized in relatively low magnetic fields. When applied to the dispersion the particles organize along chains due to magnetic dipole interaction that is attractive when the dipoles are head-to-tail and repulsive when they are side-by-side[36]. Fig. 1 shows scanning electron micrographs of aligned and cured films for Ni particles (both flakes and spheres) at selected particle concentrations. For a low particle-fraction samples (0.11 vol. %), the alignment results in particle chains, but low particle fraction leads to shorter chains (Fig. 1 a,d). When the particle fraction is increased to an intermediate level (2.5 vol. %), they remain well separated but form aligned chains long enough to run continuously through the film thickness direction (Fig. 1 b,e). Columnar structures are formed as the particle fraction is increased (Fig. 1 c,f). Morphology of non-aligned Ni particles/PDMS can be found in electronic supplementary information.

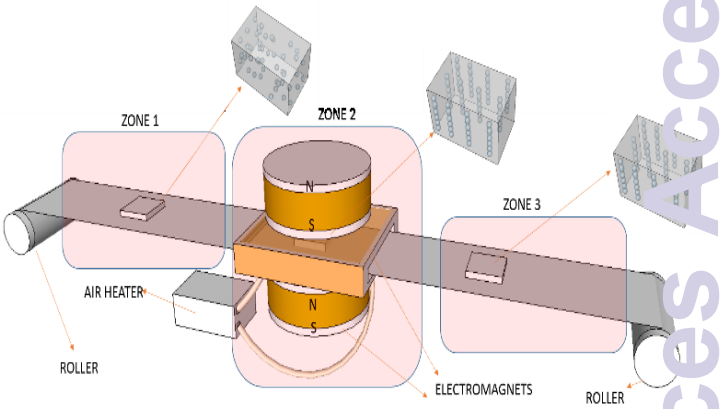

Fig. 2 A schematic model for showing the roll to roll magnetic alignment process.

As shown in Fig. 2, in the absence of external magnetic field, in the zone 1, the particles have no magnetic dipole and chains of nanoparticles (nanocolumns) do not form. In the zone 2 those Ni particles acquire a certain magnetization $M(H)$ in presence of a magnetic field H[35, 37], a behavior, governed by the particle's ferromagnetic nature. Hence they attain magnetic dipole moment m_s pointing in the direction of the applied magnetic field (which we will take as the Z axis). The strength of the magnetic interaction between particles can be

characterized by the magnetic coupling parameter Γ defined as[37],

$$\Gamma = \frac{\mu_0 m_s^{\ 2}}{2\pi d^3 k_B T}$$

The behavior of magnetized particles under external fields is controlled by the values of two parameters: the filler content ϕ_0 and magnetic coupling parameter Γ. Linear chains of magnetic particles has been found in simulations and experimentally for Γ between 40 and 3×103 and ϕ_0 < 0.15[37-39]. For lower values of Γ, an equilibrium state is possible, in which colloids aggregate in linear (nonbranched) chains with an equilibrium length given by $\sqrt{\phi_0 e^{\Gamma-1}}$ [37]. For larger values of ϕ_0 and Γ, different aggregate structures can be formed including thick chains which leads to lateral aggregation of linear chains, and more complex fibrous structures[39].

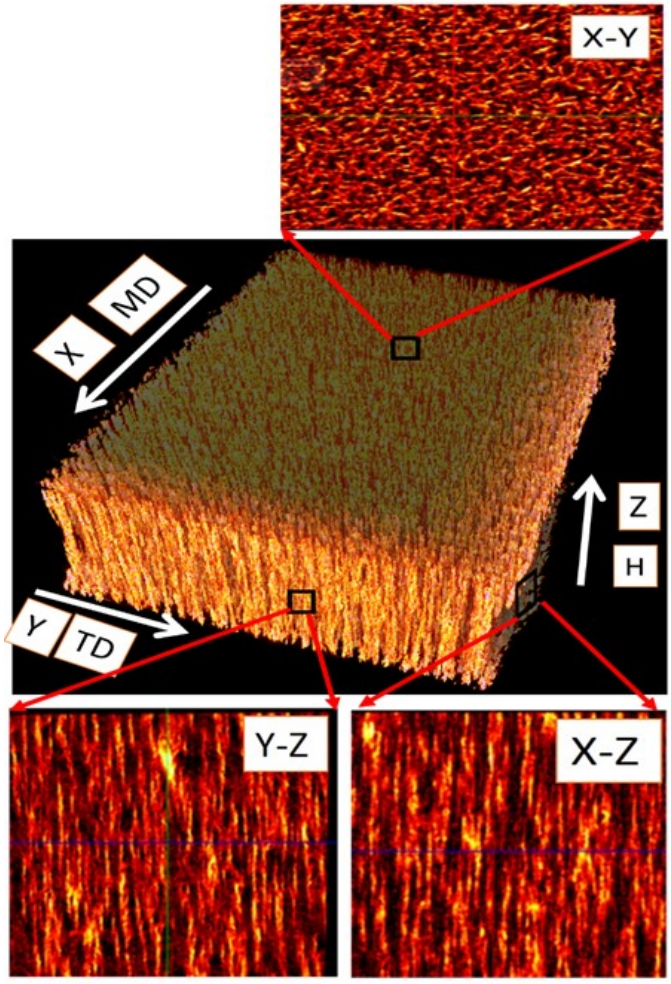

Fig. 3 Micro Computed Tomography of the preferential orientation of Ni particles (2.45vol. % Ni flakes/PDMS) through the thickness direction. (Micro-CT of non-aligned 2.45vol. % Ni flakes/PDMS available in supporting information.)

Micro-CT confirms formation of columns with their primary axes aligned in the thickness direction. As these columns span the whole thickness, they connect two surfaces while they lack connectivity in the plane as they do not exhibit any side "branches". This translates into unique and efficient "directed percolation" leading to anisotropy in electrical conductivity in these films.

Electric Conductivity Measurements

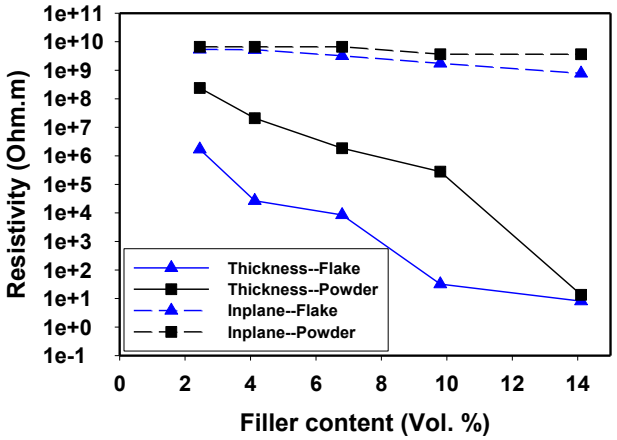

Fig. 4 Resistivity in through thickness direction of Ni/PDMS composite films

As illustrated in Fig. 4, in the film plane, the films are essentially insulating as they exhibit the same resistivity as the unfilled polymer while through thickness resistivity decreases very rapidly with particle concentration almost 9 decades with increase of 12% filler. As the filler content is increased, the resistivity of aligned Ni/PDMS films decreased drastically, as low as 10^0 ohm·m at 14 vol. %, while for non-aligned Ni/PDMS composite, the resistivity remaining greater than 10^9 ohm·m, even at 14 vol. %. Aligned Ni flake/PDMS shows lower resistivity than Ni sphere/PDMS as they form better connection (effective contact area) than spheres.

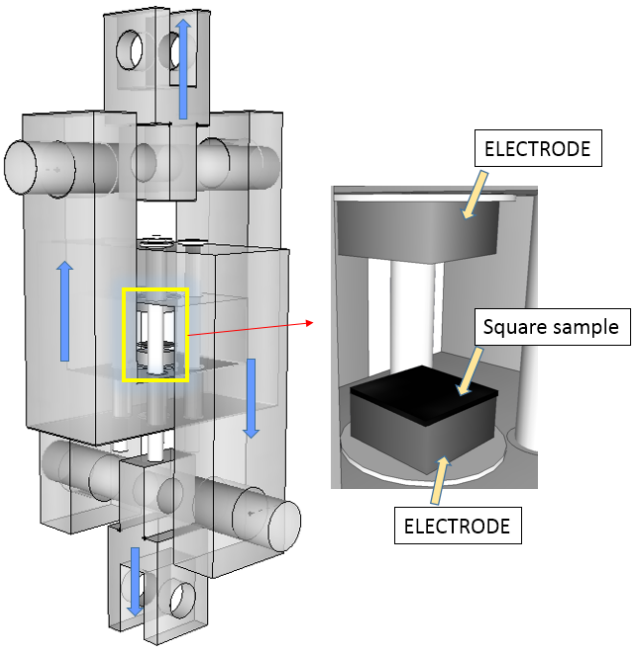

Fig. 5 Piezoresistivity measurement system.

In order to assess the piezo resistivity, we developed a custom testing system attached to a stretching device that tracks conductivity real time during compression[40]. The square sample is compressed in the device (Fig. 5) while we monitor the load on the specimen that is converted to real time pressure while conductive electrodes at the top and bottom of the sample continuously monitor the resistivity (Fig. 5), using a Keithley 6487 Picoammeter connected to a computer..

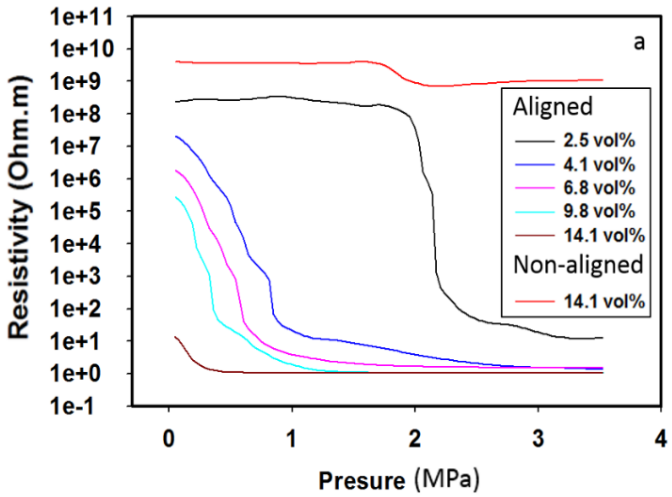

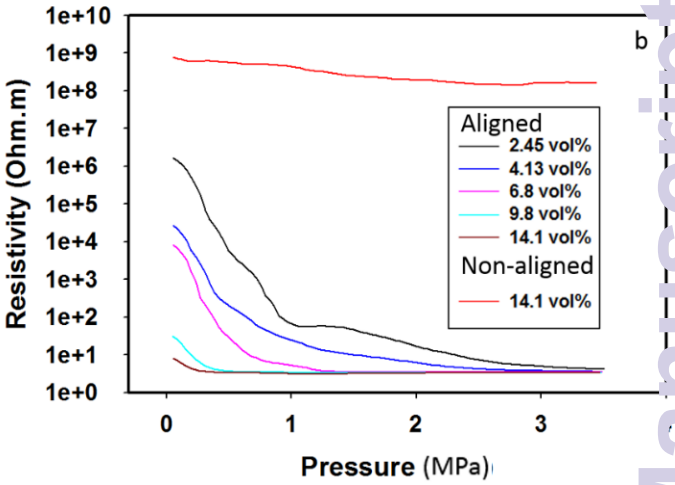

Fig. 6 Resistivity of composite in film thickness direction under compression. (a) Ni powder/PDMS; (b) Ni flake/PDMS.

The resistivity decreases dramatically with increasing pressure (Fig. 6) and eventually reaches plateau value as low as 10^0 ohm·m under 3 MPa pressure. As mentioned earlier, Ni flakes form better connection between particles, we can see the lower resistivity was observed for Ni powder/PDMS composite at the same loading. Durabilty of piezoresitivity have not yet been implemented because the our custom made device can not do cyclic compress test now.

Piezoresistivity behavior maybe described by tunneling conduction theory. In a tunneling transport process the charge carrier travel through the sample across insulating gaps between conductive particles. It has been shown that the conductivity of a composite can be reasonably well described by the behavior of a single tunnel junction. The conductance G_{ij} between two grains i and j is be expressed by equation 1[41-43],

$$G_{ij} = e^2\gamma_0 / kT \exp(-2\lambda S_{ij} - E_{ij}/kT) \quad 1)$$

Where $\lambda = (2mV(T)/h^2)^{1/2}$ is the tunneling parameter; E_{ij} is depend on electron energy at sites i and j, S_{ij} denotes the distance between the grain surface along the line joining their centers (tunneling distance). By analyzing equation 1, the relationship between resistivity and tunneling distance can be derived as[44, 45]

$$\rho(P) = \rho(0)\exp(-2\lambda\Delta d) = \rho(0)\exp(-2\lambda dP/E) \quad 2)$$

Where $\rho(P)$ is the composite resistivity under uniaxial pressure P and $\rho(0)$ is the resistivity of composite witho

pressure, d is the interparticle gap and E the Young's modulus. Thus the plot of $\ln \rho(P)$ versus P should be a straight line of slope $-2\lambda d / E$. We can see from Fig. 6 that the dependence is not linear over the range of measurement. However, a straight line can be fitted to the low-pressure data (P<0.2 MPa). Although the equation 2) is simplistic for modeling the piezoresistive behavior of aligned Ni/PDMS samples, it still captures the change in resistivity with pressure.

Fig. 6 also shows the piezoresistive behavior of the composite with various Ni concentrations. As expected, the resistivity decreases with increasing pressure, as the conducting particles are forced closer together. We note that the transition becomes sharper for composites with higher loadings of Ni. There are two main reasons for this behavior: Since the modulus of Ni is higher than PDMS, the pressure on the small gaps between Ni particles (where the tunneling takes place) is much higher than PDMS between Ni chains, that leads to a sensitive piezoresisitivity effect. Another reason for the transitions are sharper for composites with high loading, is that the number of conducting paths increase with increasing Ni loading.

Thermal Conductivity Measurements

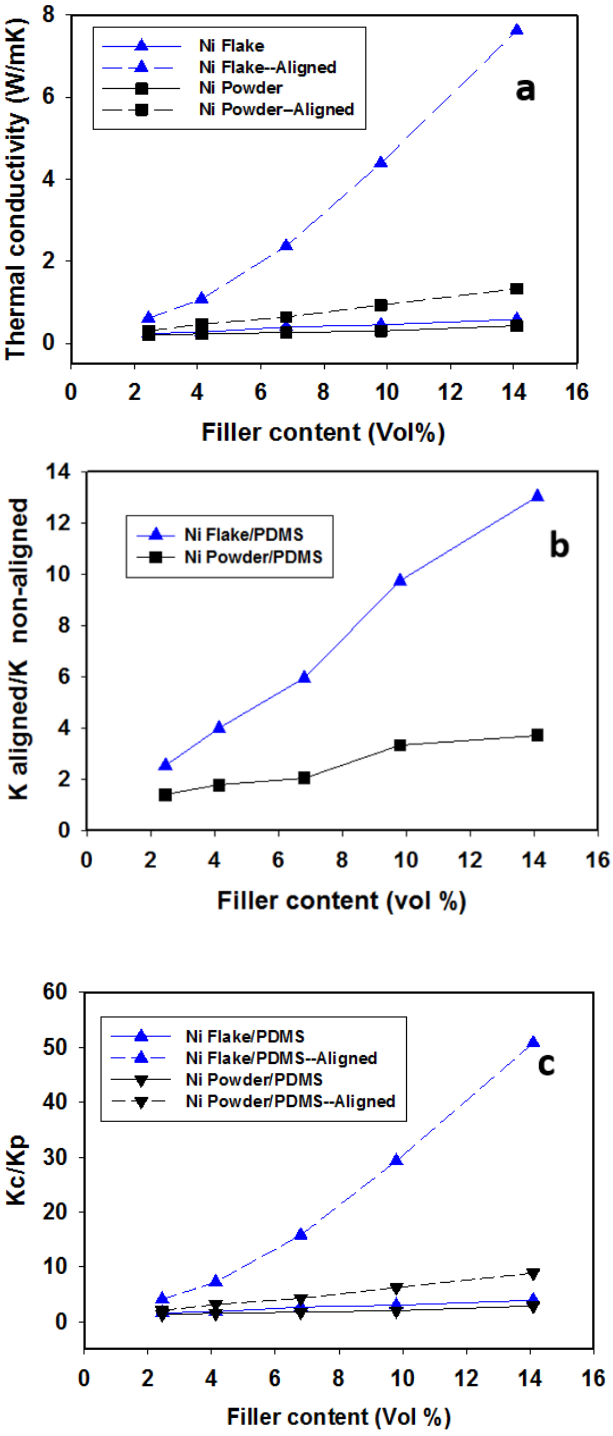

Fig. 7 a) thermal conductivity of Ni/PDMS composites; b) Kaligned/Knon-aligned; c) Kaligned/Kpolymer matrix.

The thermal conductivity of Ni/PDMS composites prepared from both particles and flakes fillers are measured over a wide range of filler loadings. Experimental data are shown in Fig. 7 as a function of volume fraction. The reported thermal conductivity are average values of 3 measurements. We can see that the thermal conductivity of non-aligned

powder/PDMS composites only increases slightly even at concentrations as high as 14 vol. % (60 wt. %) Ni loading, while for aligned Ni powder/PDMS composites, the thermal conductivity increases as Ni sphere loading is increased (Fig. 7 a), as high as 3.5 times of non-aligned one (Fig. 7 b). This occurs as the connected paths created by the Ni powder chains lead to efficient thermal transfer channels through polymer matrix. Once the Ni chains are formed, the thermal conductivity of composite increases drastically along the chain direction. We also can see, the thermal conductivity of field aligned composite film filled with 14 vol.% Ni flakes is as high as 50 times the conductivity of polymer matrix, or 13 times the conductivity of non-aligned composite containing the same concentration of conductive filler (Fig. 7 c). The effective contact area between powders is small as we show in Fig. 4 b, the flakes with a high aspect ratio are particularly effective in providing good particle-to-particle contact to efficient heat transfer.

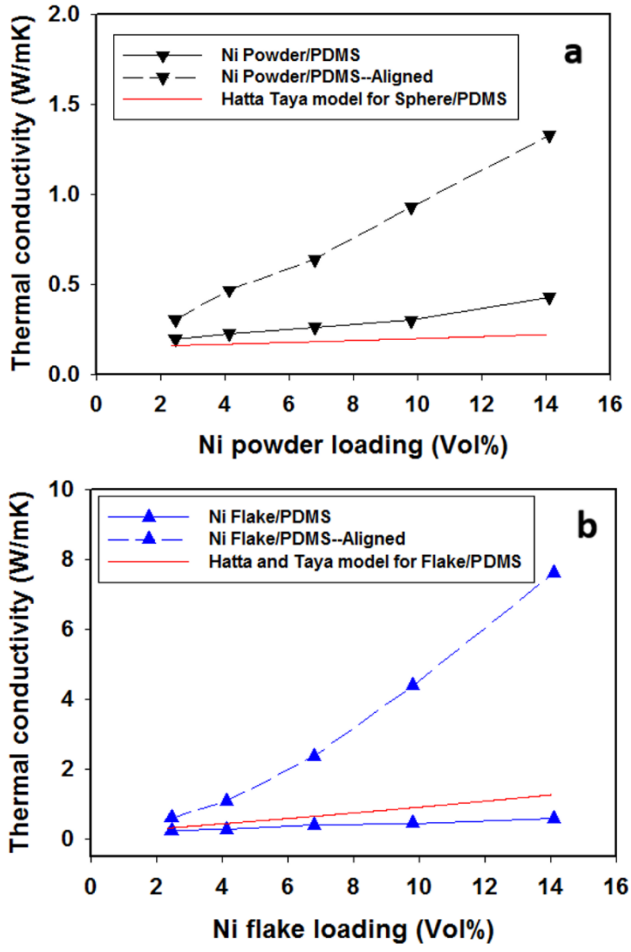

Fig. 8 Comparison of experimentally data with Hatta and Taya model. a) sphere model, b) flake model.

Hatta and Taya[46, 47] used an equivalent inclusion method to develop a model for the prediction of heat conduction in two-phase composites according to the equation.

$$K_{c,i} = K_p + \frac{\phi(K_f - K_p)K_p}{(K_f - K_p)(1-\phi)S_i + K_p}$$

where $K_{c,i}$ is the thermal conductivity of the composite along one defined axis direction, i ($i = x, y, z$), and S_i the factor dependent on filler shape and direction.

For sphere, $S_x = S_y = S_z = \frac{1}{3}$

For flakes, for measurements made parallel to the plane of aligned platelets in a composite, (defined as the x- and y-directions), for measurements made perpendicular to the plane of aligned flakes in a composite, defined as the z-direction.

$$S_x = S_y = \frac{\pi T}{4D} \quad S_z = 1 - \frac{\pi T}{2D}$$

In this paper, for Ni powder/PDMS, S=1/3; for Ni flake/PDMS, T=1um, D=37um, S=0.02. Model prediction is also plotted in Fig. 8. The experimental data for the non-aligned Ni powder/PDMS composite exceed the model's prediction (Fig. 8 a), because the Ni powder we used is not perfect sphere, they have spiky surfaces with high aspect ratio (See SEM images in supporting information), which increase the thermal conductivity. For the aligned Ni powder/PDMS composites, the experimental data is greater, that is because Hatta and Taya model does not consider chain structure formation, which provide efficient heat conduction pathway through thickness direction. In this structure the chains increase the effective length of the thermal path through the particles uninterrupted by thick polymer interfaces, thus, in turn, enhances the thermal conductivity. Since the Hatta and Taya model considers orientation without chain formation, the model's prediction for Ni flake/PDMS should be greater than the experimental data of Non-aligned (No chains and No orientation) and lower than aligned Ni flake/PDMS composites, which were demonstrated in our experiment data. (Fig. 8 b)

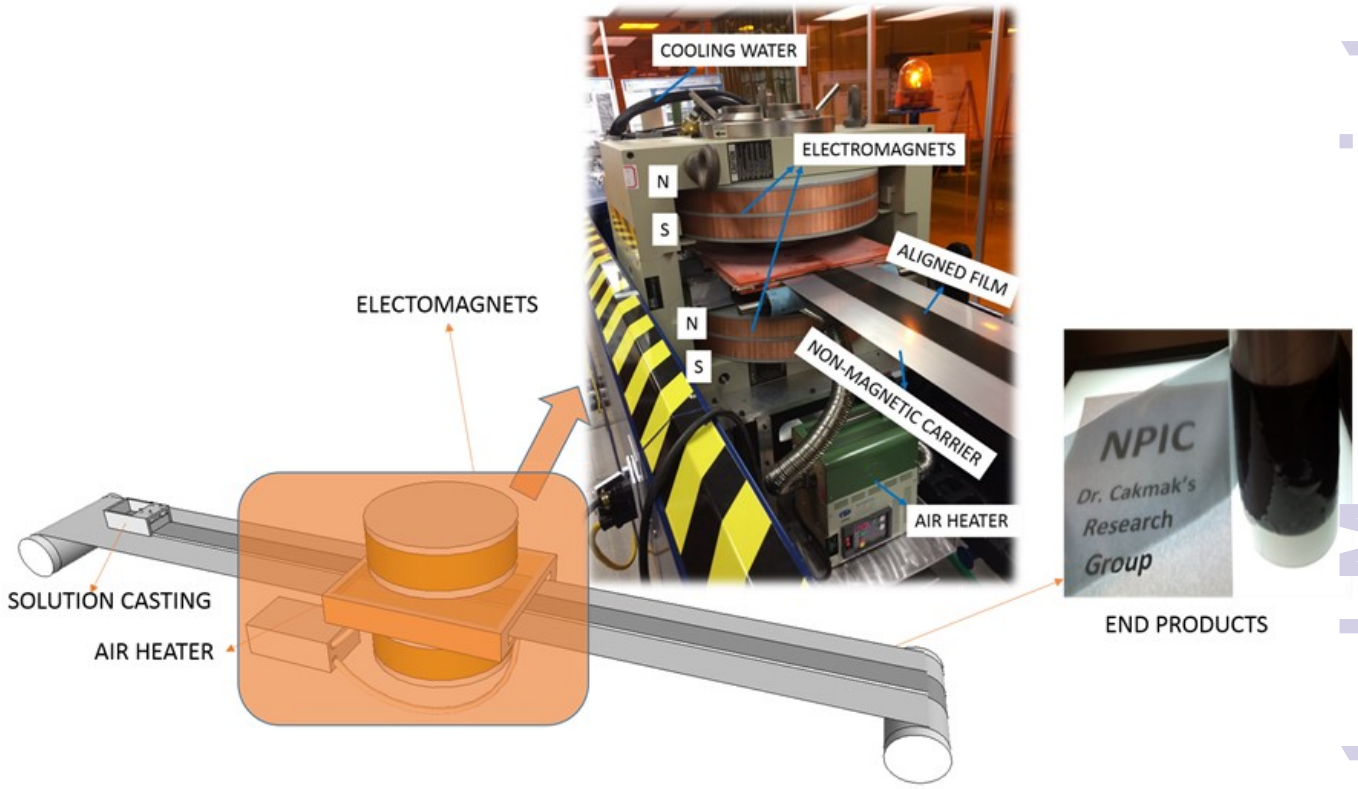

Fig. 9 A schematic model for showing the roll to roll magnetic alignment process.

Fig. 9 shows the schematic of 70 feet roll to roll manufacturing line with in-line electromagnet. In this process, the solution premixed with nanoparticles is cast on to a carrier polymer film using a double doctor blade casting system with a desired solution thickness. As the film carrying this solution is transported by the carrier it enters the gap between the poles of the electromagnet. The magnetic field inside this gap is reasonably uniform measured and reported earlier. 5 In this process, the nanoparticles are organized along columns made up of nanoparticles. The PDMS is thermally cured while the film is inside the magnetic field as it is transported along the machine direction. (Video available in supporting information.)

To establish that the magnetic field induced alignment can be accomplished using the roll-to-roll setup with realistic manufacturing conditions, we were able to cast films of oriented Ni flake and Ni powder (3" wide and 200" long) nanocomposites at 2.5 vol. % filler concentration with applied strength of 200mT at 5 cm/min speed. Ni /PDMS film aligned by magnetic field shows high optic transmittance than the non-aligned one's as show in Fig. 10. SEM proved the anisotropic structure as shown in Fig. 10 and Figure 11. More importantly, optical transmittance of aligned samples show dependence on incident angle (Fig. 12). As the nanoparticle columns form and grow into long chains, they also "sweep" all the particles between them creating particle free depletion zones that run through the thickness direction. When light is shone with the incidence angle of 0°, it passes through these "clear" pathways and hence we achieve reasonable transparency at higher loadings. Because the columns of nanoparticles that are oriented in and span the thickness direction off normal angles lead to absorption of light as illustrated in the Fig. 12.

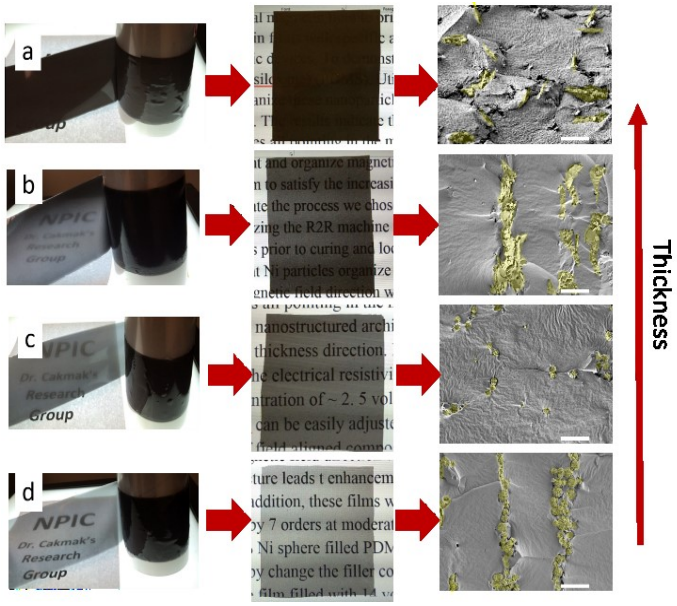

Fig. 10 Optical transmittance of Ni/PDMS film. a), 2.5vol. % Ni flake/PDMS Non-aligned b), 2.5vol. % Ni flake/PDMS Aligned c), 2.5vol. % Ni powder/PDMS Non-aligned d), 2.5vol. % Ni powder/PDMS Aligned. (Scale bar: 20um)

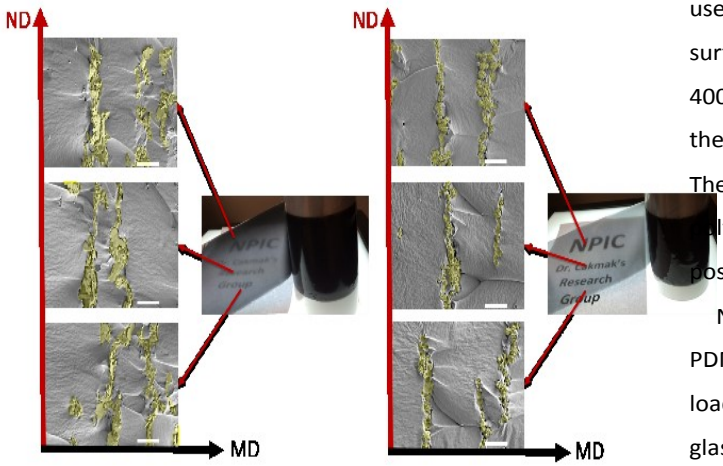

Fig. 11 Ni particles aligned in PDMS by roll to roll process. (Scale bar: 20 um)

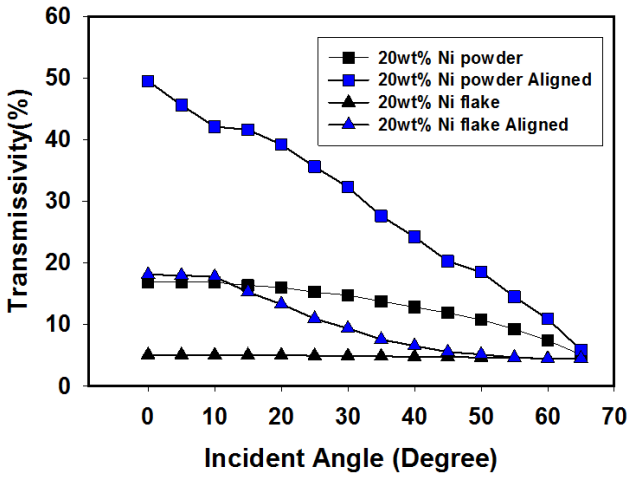

Fig. 12 Incident angle dependence of optical transmittance.

Experimental

Sylgard 184 Silicone Elastomer base and curing agent was purchased from Dow Corning Corporation and used as obtained. Ni powders and flakes (Type 123 and HCA-1 were kindly provided Novamet Specialty Products Corp. USA) and used as received. Ni powders have a characteristic spiky surface and a particle size of 3–6µm. Ni Flakes have average 400 mesh diameter and 1um thickness. Both the matrix and the fillers were used as is without any further modifications. The PDMS resin was chosen since it is liquid and heat curable polymer, thus making the mixing and fixing the alignment possible.

Ni powders and flakes were mixed and defoamed with PDMS by Thinky planetary vacuum mixer at varied particle loadings. For the square samples, the blends was casted into glass cell then cured by 150 C hot air 30 mins, the thickness of samples are 1cm, while for long film the blends was casted by doctor blade on the substrate carried by the stainless steel belt by roll to roll processing line[5], the magnetic and hot air were applied when the film passing by two poles of the electromagnet assembled on the machine, the thickness of roll films are 0.2 mm. The roll to roll speed set at 5 cm/min, at the same time, 150 C hot air was applied to cure the PDMS resin, it took around 5 min to pass through electromagnets(200 mT) that was enough to cure 0.2 mm PDMS film at 150 C.

The morphology of cured films was characterized using scanning electron microscope (JEOL JSM 5310) and Skyscan 1172 Micro Computed Tomography Scanner.

Piezoresistivity was real-time tested under increasing pressure by homemade machine named A2, which can measure electric current as fast as 100 scans per second. Samples were placed between two aluminum plates. The resistance measurements were carried out using a Keithley 6487 Picoammeter. A uniaxial pressure was applied perpendicular to the planes of test samples (along the thickness direction) to get a good conductive contact.

Thermal conductivity were measured by FOX 50 Series Thermal Conductivity Analyzer.

Conclusions

We have demonstrated a novel R2R process with magnetic field assisted alignment technique to fabricate vertically oriented Ni particles along nanocolumns in a flexible polymer matrix which exhibits very high electrical and thermal conductivities in thickness direction. Piezoresistivities of anisotropic polymer composite films was analyzed with aligned particle inside by real-time compression test method and found that range and sensitivity of polymer composite film properties can be tuned by particle loading. This is the first successful scale-up of the alignment of Ni particles in polymers on a prototype custom-built 70 ft X1 ft R2R machine with electromagnets units, thus designing polymer composites with anisotropic electric, thermal, optical and mechanical properties. These anisotropic films can be used for a wide range of applications such as touch sensors, “Z direction “heat spreaders, and privacy protection films.

Acknowledgements

This work was financially supported by Third frontier of state of Ohio that provided funding to develop the roll to roll manufacturing line. In addition the authors gratefully acknowledge the doctoral innovation fund and scholarship of Donghua University and China scholarship council.

Notes and references

1. J. R. Lu, W. G. Weng, X. F. Chen, D. J. Wu, C. L. Wu and G. H. Chen, *Advanced functional materials*, 2005, 15, 1358-1363.
2. H. Høyer, M. Knaapila, J. Kjelstrup-Hansen, X. Liu and G. Helgesen, *Applied Physics Letters*, 2011, 99, 213106.
3. A. Oliva-Avilés, F. Avilés and V. Sosa, *Carbon*, 2011, 49, 2989-2997.
4. J. A. Beardslee, B. Sadtler and N. S. Lewis, *ACS nano*, 2012, 6, 10303-10310.
5. M. Cakmak, S. Batra and B. Yalcin, *Polymer Engineering & Science*, 2015, 55, 34-46.
6. C. Martin, J. Sandler, A. Windle, M.-K. Schwarz, W. Bauhofer, K. Schulte and M. Shaffer, *Polymer*, 2005, 46, 877-886.
7. J. Ramón‐Azcón, S. Ahadian, M. Estili, X. Liang, S. Ostrovidov, H. Kaji, H. Shiku, M. Ramalingam, K. Nakajima and Y. Sakka, *Advanced Materials*, 2013, 25, 4028-4034.
8. F. Du, J. E. Fischer and K. I. Winey, *Physical Review B*, 2005, 72, 121404.
9. S. U. Khan, J. R. Pothnis and J.-K. Kim, *Composites Part A: Applied Science and Manufacturing*, 2013, 49, 26-34.
10. H. Wang, H. Zhang and G. Chen, *Composites Part A: Applied Science and Manufacturing*, 2007, 38, 2116-2120.
11. T. Kimura, H. Ago, M. Tobita, S. Ohshima, M. Kyotani and M. Yumura, *Advanced materials*, 2002, 14, 1380-1383.
12. E. Sancaktar and N. Dilsiz, *Journal of adhesion science and technology*, 1999, 13, 679-693.
13. M. V. Jose, B. W. Steinert, V. Thomas, D. R. Dean, M. A. Abdalla, G. Price and G. M. Janowski, *Polymer*, 2007, 48, 1096-1104.
14. D. Wang, P. Song, C. Liu, W. Wu and S. Fan, *Nanotechnology*, 2008, 19, 075609.
15. E. Moaseri, M. Karimi, M. Baniadam and M. Maghrebi, *Composites Part A: Applied Science and Manufacturing*, 2014, 64, 228-233.
16. N. Li, G.-W. Huang, H.-M. Xiao and S.-Y. Fu, *Composites Part A: Applied Science and Manufacturing*, 2015, 77, 87-95.
17. P. Goh, A. Ismail and B. Ng, *Composites Part A: Applied Science and Manufacturing*, 2014, 56, 103-126.
18. S. G. Prolongo, B. G. Meliton, G. Del Rosario and A. Ureña, *Composites Part B: Engineering*, 2013, 46, 166-172.
19. B. Z. Tang and H. Xu, *Macromolecules*, 1999, 32, 2569-2576.
20. C. Mao, J. Huang, Y. Zhu, W. Jiang, Q. Tang and X. Ma, *The Journal of Physical Chemistry Letters*, 2012, 4, 43-47.
21. H. Wu, J. Liu, X. Wu, M. Ge, Y. Wang, G. Zhang and J. Jiang, *International journal of adhesion and adhesives*, 2006, 26, 617-621.
22. S. Darling, *Progress in Polymer Science*, 2007, 32, 1152-1204.
23. Y. Lin, A. Böker, J. He, K. Sill, H. Xiang, C. Abetz, X. Li, J. Wang, T. Emrick and S. Long, *Nature*, 2005, 434, 55-59.
24. B. Sohn and B. Seo, *Chemistry of materials*, 2001, 13, 1752-1757.
25. P. W. Majewski, M. Gopinadhan, W.-S. Jang, J. L. Lutkenhaus and C. O. Osuji, *Journal of the American Chemical Society*, 2010, 132, 17516-17522.
26. M. Gopinadhan, P. W. Majewski and C. O. Osuji, *Macromolecules*, 2010, 43, 3286-3293.
27. A. Anwer and A. Windle, *Polymer*, 1993, 34, 3347-3357.
28. S. A. Kossikhina, T. Kimura, E. Ito and M. Kawahara, *Polymer engineering and science*, 1998, 38, 914.
29. M. Gopinadhan, P. W. Majewski, E. S. Beach and C. O. Osuji, *ACS Macro Letters*, 2011, 1, 184-189.
30. C. Osuji, P. J. Ferreira, G. Mao, C. K. Ober, J. B. Vander Sande and E. L. Thomas, *Macromolecules*, 2004, 37, 9903-9908.
31. T. Pullawan, A. N. Wilkinson and S. J. Eichhorn, *Biomacromolecules*, 2012, 13, 2528-2536.
32. E. Choi, J. Brooks, D. Eaton, M. Al-Haik, M. Hussaini, H. Garmestani, D. Li and K. Dahmen, *Journal of Applied physics*, 2003, 94, 6034-6039.
33. S. Jin, T. Tiefel and R. Wolfe, *Magnetics, IEEE Transactions on*, 1992, 28, 2211-2213.
34. S. Jin, R. Sherwood, J. Mottine, T. Tiefel, R. Opila and J. Fulton, *Journal of Applied Physics*, 1988, 64, 6008-6010.

35. J. S. Andreu, C. Calero, J. Camacho and J. Faraudo, *Physical Review E*, 2012, 85, 036709.
36. J. W. Swan, P. A. Vasquez, P. A. Whitson, E. M. Fincke, K. Wakata, S. H. Magnus, F. De Winne, M. R. Barratt, J. H. Agui and R. D. Green, *Proceedings of the National Academy of Sciences*, 2012, 109, 16023-16028.
37. J. Faraudo, J. S. Andreu and J. Camacho, *Soft Matter*, 2013, 9, 6654-6664.
38. P. Domínguez-García, S. Melle, J. Pastor and M. Rubio, *Physical Review E*, 2007, 76, 051403.
39. M. Fermigier and A. P. Gast, *Journal of colloid and interface science*, 1992, 154, 522-539.
40. T. L. Kwa, University of Akron, 2006.
41. P. Sheng and J. Klafter, *Physical Review B*, 1983, 27, 2583.
42. M. Mehbod, P. Wyder, R. Deltour, C. Pierre and G. Geuskens, *Physical Review B*, 1987, 36, 7627.
43. V. K. S. Shante, *Physical review B*, 1977, 16, 2597.
44. T. A. Ezquerra, M. Kulescza, C. S. Cruz and F. J. Baltá‐Calleja, *Advanced Materials*, 1990, 2, 597-600.
45. J. Dawson and C. Adkins, *Journal of Physics: Condensed Matter*, 1996, 8, 8321.
46. H. Hiroshi and T. Minoru, *International Journal of Engineering Science*, 1986, 24, 1159-1172.
47. R. F. Hill and P. H. Supancic, *Journal of the American Ceramic Society*, 2002, 85, 851-857.